ACS SyntheticBiology

Research Article

pubs.acs.org/synthbio

Probing Cell-Free Gene Expression Noise in Femtoliter Volumes

David K. Karig,[†] Seung-Yong Jung,[‡] Bernadeta Srijanto,[†] C. Patrick Collier,[†] and Michael L. Simpson*[,†,§,⊥]

[†]Center for Nanophase Materials Sciences, Oak Ridge National Laboratory, Bethel Valley Road, Oak Ridge, Tennessee 37831, United States

[‡]Biosciences Division, Oak Ridge National Laboratory, Oak Ridge, Tennessee 37831, United States

[§]Department of Materials Science and Engineering, University of Tennessee, Knoxville, Tennessee 37996-2010, United States

[⊥]Center for Environmental Biotechnology, University of Tennessee, Knoxville, Tennessee 37996-2010, United States

Supporting Information

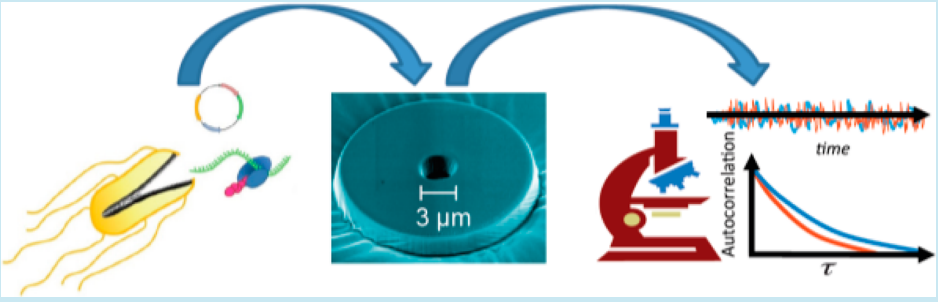

ABSTRACT: Cell-free systems offer a simplified and flexible context that enables important biological reactions while removing complicating factors such as fitness, division, and mutation that are associated with living cells. However, cell-free expression in unconfined spaces is missing important elements of expression in living cells. In particular, the small volume of living cells can give rise to significant stochastic effects, which are negligible in bulk cell-free reactions. Here, we confine cell-free gene expression reactions to cell-relevant 20 fL volumes (between the volumes of *Escherichia coli* and *Saccharomyces cerevisiae*), in polydimethylsiloxane (PDMS) containers. We demonstrate that expression efficiency varies widely among different containers, likely due to non-Poisson distribution of expression machinery at the observed scale. Previously, this phenomenon has been observed only in liposomes. In addition, we analyze gene expression noise. This analysis is facilitated by our use of cell-free systems, which allow the mapping of the measured noise properties to intrinsic noise models. In contrast, previous live cell noise analysis efforts have been complicated by multiple noise sources. Noise analysis reveals signatures of translational bursting, while noise dynamics suggest that overall cell-free expression is limited by a diminishing translation rate. In addition to offering a unique approach to understanding noise in gene circuits, our work contributes to a deeper understanding of the biophysical properties of cell-free expression systems, thus aiding efforts to harness cell-free systems for synthetic biology applications.

KEYWORDS: *cell-free expression, confinement, noise, stochastic*

INTRODUCTION

Cell-free systems have found wide use in biological studies including the characterization of membrane proteins,[1] the probing of protein interactions,[2] and the exploration of fundamental aspects of translation.[3,4] Here we use cell-free protein expression reactions to study stochasticity in gene expression in a simplified context. Gene expression in living cells is inherently stochastic due to small cell volumes and the fact that many important reactants are present in small numbers.[5] This inherent noise has been shown to play a key role in numerous biological processes.[6−8] Living cells have evolved to minimize noise in some cases and harness it in others.[9,10] For example, negative feedback, which is a common motif in bacterial gene networks, can push noise to higher frequencies, where it can be more easily filtered.[11,12] On the other hand, noise has also been implicated in the HIV decision between active replication and latency,[13] the λ phage decision between lysis and lysogeny,[14,15] and the *Bacillus subtillus* decision between competence and sporulation.[15] In addition, noise can offer advantages to a population of cells exposed to environmental stress.[16] Analysis of gene expression noise can shed light on the architecture of gene circuits and the organization of gene networks,[14,15] can help to determine kinetic parameters,[17−19] and can yield insights into the construction of synthetic gene networks.[20,21]

However, studying noise in living cells is complicated due to the multiple sources of noise. Besides stochasticity in gene expression, microenvironment variation, volume changes due to cell growth,[22] random partitioning of cell contents upon

Received: March 13, 2013
Published: May 20, 2013

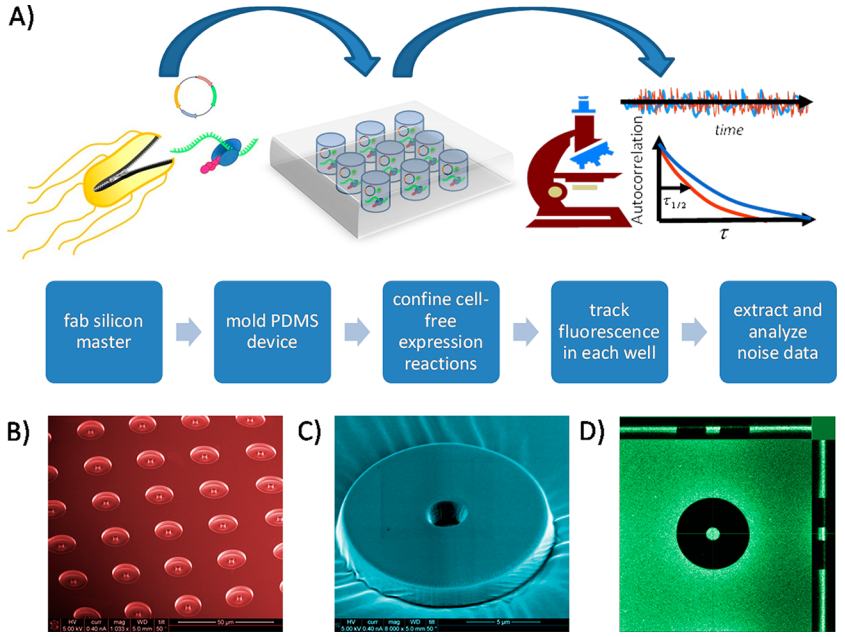

Figure 1. (A) Cell-free gene circuit reactions are confined in nanofabricated fL scale devices for the purpose of quantifying gene expression noise. First, devices are created by fabricating a silicon master. The silicon master is used to mold an array of PDMS wells. Cell-free protein expression reactions are then confined in the PDMS wells. Fluorescence of the confined reactions is tracked over time for each well using fluorescent microscopy, and gene expression noise is extracted and characterized. (B) Silicon mold for making PDMS devices. (C) PDMS container with a 3 μm diameter inner well. (D) 3D orthogonal profile view of GFP mixed with cell extract and loaded into a PDMS container with a 7 μm diameter inner well.

division,[23] differences in cell−cell contacts,[24] epigenetic variation,[25,26] and mutation contribute to population variability. This makes it challenging to distinguish intrinsic noise arising from the probabilistic reactions of the gene circuit of interest from extrinsic noise arising from environmental fluctuations.[27] Cell-free protein expression reactions offer the opportunity to study stochasticity in gene expression in a simplified context. In particular, because cell-free systems avoid many of the complicating factors (cell division, etc.) contributing to noise in living cells, the majority of noise in cell-free systems can be attributed to the gene expression itself.

Cell-free systems are also more flexible than living cells. While this can be beneficial in certain contexts, it also means that typical cell-free preparations differ from living cells in terms of composition and biophysical properties. For example, many cell-free preparations are optimized to improve mRNA and protein stability. Also, crowding is usually achieved through the addition of artificial crowding agents such as polyethylene glycol. Recent studies have sought to mimic the cytoplasmic environment[28] and to achieve crowding without artificial reagents.[29] However, this might not be desirable in all circumstances. Indeed, one of the most important benefits of cell-free systems is that they can be formulated to examine parameter spaces that either mimic the cell or that extend far beyond what is realized in cells. In this contribution, we capitalize on the simplicity and flexibility offered by cell-free systems to study intrinsic noise in a simple constitutive expression system.

While the simplicity of cell-free systems makes them ideal for characterization of noise in gene expression reactions, care must be taken to ensure that the scale of gene expression noise in cell-free systems matches that in living cells. In this respect, a key requirement for quantifying the inherent stochasticity of gene network architectures is to confine reactions in sufficiently small volumes. For a given set of reactant concentrations, as reaction volume decreases stochastic effects generally become more pronounced due to the smaller numbers of reactant molecules in the system. Moreover, other system properties besides stochasticity also change with size. As volume decreases, the surface area to volume ratio increases, which facilitates interactions with the external environment and can also lead to internal phenomena such as adsorption and surface localization of reactants.[30,31] Most cell-free systems that have been explored to date are too large to exhibit significant stochasticity or other small-volume effects.

A few efforts have achieved small-volume confinement of cell-free expression reactions in liposomes. For example, Nomura et al. demonstrated expression in vesicles that were approximately 5 μm in diameter but did not study gene expression noise.[32] Nourian and Danelon examined the distributions of DNA and two different fluorescent proteins in liposomes of assorted sizes but did not quantify the dynamics of noise.[33] Also, de Souza et al. demonstrated expression in vesicles that were 200 nm in diameter, but expression in individual vesicles could not be measured.[34] Besides vesicles, another approach is confinement in fabricated containers. These offer the benefit of precisely defined dimensions; however, there has been very limited small-volume confinement in fabricated containers. Recently, Okano et al. achieved expression from single DNA molecules in glass microchambers ranging from 40 fL to 7 pL, but single-well kinetics were only presented for the larger 7 pL wells.[35] These larger picoliter-scale volumes are representative of mammalian cell volumes, but mammalian cells feature subcompartmentalization along with slow events such chromatin remodeling that give rise to significant noise in gene expression in spite of larger overall sizes.[36] Since we aim to study simpler bacterial expression using *Escherichia coli* extracts, achieving smaller fL scale volumes is

dx.doi.org/10.1021/sb400028c | *ACS Synth. Biol.* 2013, 2, 497−505

critical to recreating the context in which stochasticity operates in cells.

As illustrated in Figure 1A, we confine cell-free gene expression reactions in PDMS containers of volumes down to 20 fL, which is between the approximately 1 fL volume of *E. coli*[37] and the 60 fL volume of *Saccharomyces cerevisiae*.[38] To confine cell-free expression reactions, we first fabricate silicon masters as shown in Figure 1B. These are used to mold arrays of PDMS gaskets such as the one shown in Figure 1C. To load the resulting PDMS device, reagents are dispensed onto microscope cover glass, and the PDMS device is forced down onto the cover glass to seal reagents into the microwells. Previously, approaches in which reagents are trapped between cover glass and PDMS microwells have been applied to confine simple biochemical reactions to fL scale volumes.[39,40] However, the viscous nature of cell extracts and the presence of protein aggregates can complicate proper sealing of wells. Our gasket design, illustrated in Figure 1B–C, helps to overcome these issues by promoting proper contact between the cover glass and the PDMS immediately surrounding the microwell. In addition, the fact that reagents surround each gasket helps to prevent drying, which is a common issue for long duration experiments at the high surface area to volume ratio associated with the cellular scale.

Using our PDMS devices, we then demonstrate GFP expression from a T7 promoter in cell-sized volumes. Finally, using time-series images of confined GFP, we demonstrate quantification of the fluorescence intensity of each well, and show how this can be used for analysis of the noise properties of gene expression. Although we observe some degree of variation among different experiments at the cellular scale, several key observations revealed by noise analysis are common to all experiments. First, although typical cell-free translation rates are considerably weaker than in cells, we identify signatures of translational bursting in the noise. Second, although bursting is seen initially, the noise dynamics suggest that overall expression is limited by a diminishing translational burst rate. Thus, in addition to offering a novel approach to studying gene expression noise, our work reveals important properties and kinetics of cell-free expression at the microscale.

RESULTS AND DISCUSSION

Cell-free protein expression systems facilitate research at the interface of chemistry and biology, as they offer the ability to probe and perturb the underlying machinery of the cell in ways that are difficult or impossible in living cells. The further confinement of cell-free reactions in nanofabricated devices yields well-defined platforms for studying the effects of key cell properties such as size, shape, and molecular crowding on reaction dynamics and noise. In this study, we performed a series of experiments aimed at probing intrinsic noise properties of gene expression through the use of cell-free systems. First, we conducted a set of experiments to characterize the device setup and to verify proper loading and sealing of reagents. Specifically, we mixed purified EGFP with cell extract, loaded the devices, and captured Z-stack images. Figure 1D shows a 3D orthogonal view clearly illustrating that the wells are fully filled. Figure 2A depicts multiple adjacent wells. These confocal Z-stacks show that the wells are also filled evenly. To demonstrate that proper sealing of the devices can be achieved, we conducted FRAP (fluorescence recovery after photobleaching) experiments. For example, in Figure 2B, half of a 7 μm diameter well was bleached. Even though only half of

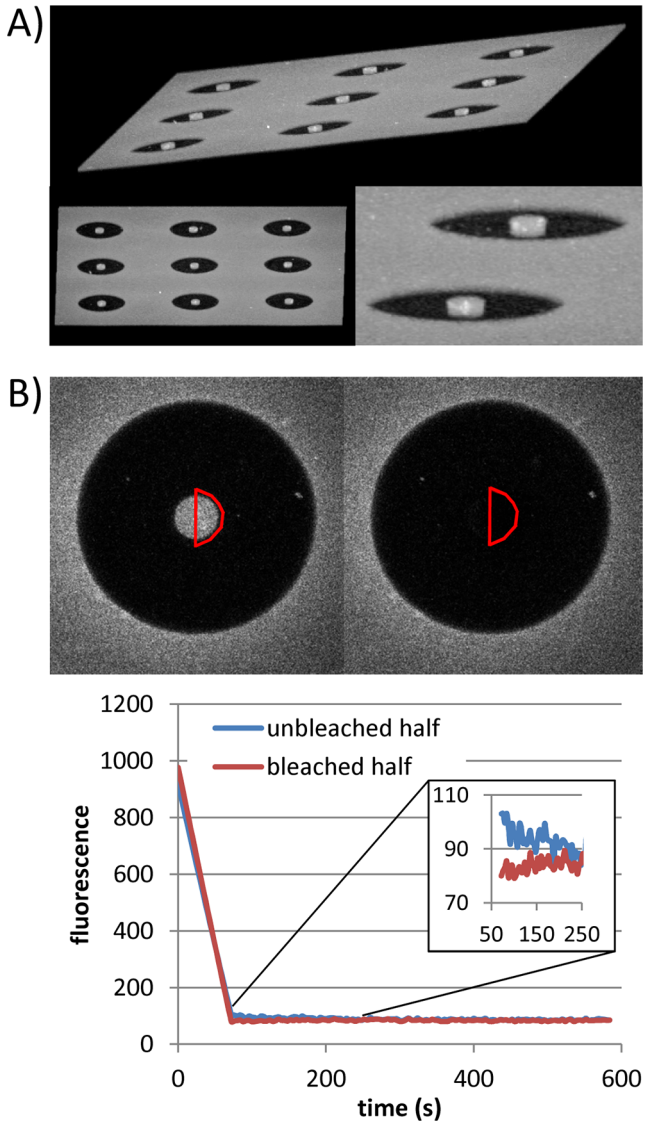

Figure 2. (A) Confocal Z-stack renderings of purified GFP mixed with cell extract and loaded into 7 μm wells. (B) Half of a 7 μm diameter well is excited (red region in top left), yet GFP in the entire well is bleached (top right), verifying that the well has not dried. The inset reveals a slightly higher fluorescence in the unbleached portion of the well due to a small amount of GFP adsorption to the well surface.

the well was excited by the laser, fluorescence decreased in both sides of the well, which verifies that the contents are not dried out and that mixing is occurring within the well. Fluorescence is only slightly brighter in the unbleached half of the well, showing that adsorption of EGFP to the PDMS surface is minimal.

After performing basic device characterizations, we proceeded to quantify expression dynamics using devices with 3 μm diameter wells. We expressed EGFP from a T7 promoter using the genetic construct shown in Figure 3A, and we captured images every 5 min as shown in Figure 3B. Following each expression experiment, we conducted a FRAP experiment to verify proper sealing of the wells (Figure S1A in Supporting Information [SI]). We then analyzed each series of images from the expression experiments that exhibited the best sealing (experiments, A, B, and C). Before examining expression within the 3 μm wells, we first examined bulk expression dynamics by

dx.doi.org/10.1021/sb400028c | *ACS Synth. Biol.* 2013, 2, 497–505

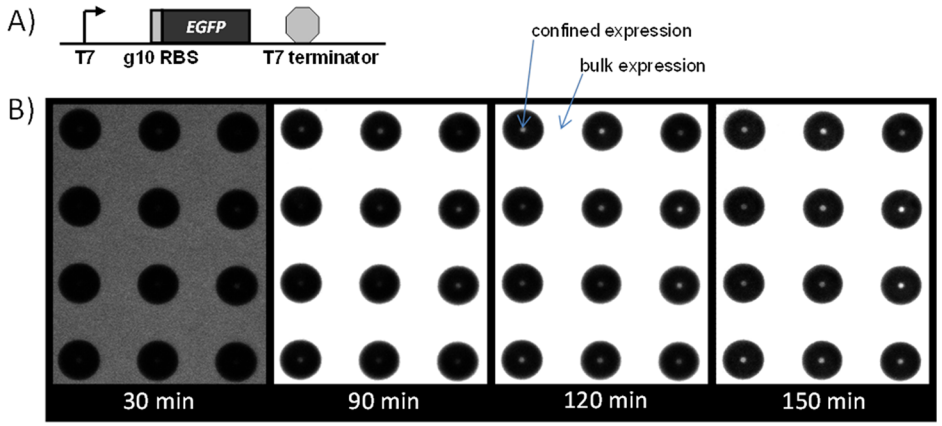

Figure 3. Expression experiments. (A) Plasmid used in expression experiments. A T7 promoter was used to express EGFP with a strong ribosome binding site, g10 RBS. A T7 terminator was used for transcription termination. (B) Sample images from an expression experiment. Images were acquired every 5 min. This enabled the quantification of confined expression within each well as well as that of unconfined bulk expression in the region surrounding the wells.

quantifying fluorescence intensity in the region surrounding the PDMS wells (Figure S1B, SI). Experiments A and B, which were conducted from the same batch of cell extract, exhibit similar bulk expression dynamics. Even though the expression was weaker for the different cell extract batch used in experiment C, normalizing each expression trajectory to its maximum level reveals that all experiments exhibit similar trends (Figure S1C, SI). In general, the cell-free expression profiles are marked by an initial delay that corresponds to the transcription of the first mRNA molecules, a strong increase in expression while transcription and translation are both active, an eventual plateauing as expression rates decrease due to reagent depletion and waste product generation, and a final decay of protein product.

After characterizing bulk expression dynamics, we then quantified expression within each PDMS well in order to study the effect of confinement on cell-free expression dynamics (Figure 4). Although the bulk dynamic trends were similar among the different experiments, we observed differences in the confined expression dynamics. For example, in experiment A (Figure 4A), fluorescence rises gradually for approximately 150 min and then plateaus. In experiment B (Figure 4B), expression rises rapidly over the first 80 min and eventually decreases. Interestingly, experiment C (Figure 4C) appears to exhibit a combination of the trends observed in experiments A and B, where some wells show a gradual increase in fluorescence while others show a rapid rise and eventual decrease in fluorescence. These differences are likely attributed to different transcription rates, since transcription dictates the initial rate at which overall expression proceeds. The fact that experiment C exhibits some traces (Cluster 1) that are similar to the experiment A profile and some (Cluster 2) that are similar to the experiment B profile suggests that transcriptional machinery is not well mixed and that different wells have different transcriptional efficiencies.

In addition to qualitative variation in expression efficiency across different experiments, we also observed significant quantitative variation between wells in each experiment. This is particularly interesting, because it hints at fundamental issues associated with cell-size confinement of cellular reactions. Potential causes for the variation are aggregation of important reagents or incomplete mixing of reagents at the micro scale. The fact that we used high DNA concentrations in our

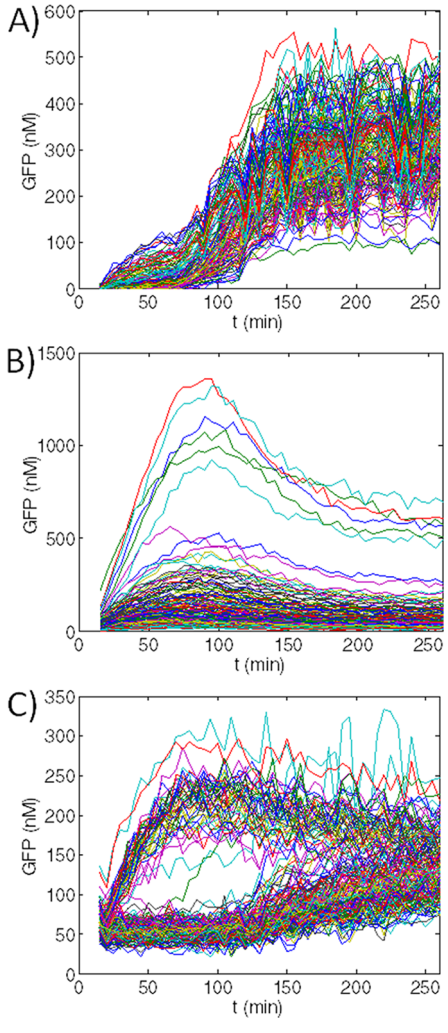

Figure 4. Fluorescence from GFP expression in 20 fL wells was tracked over time for three different experiments: (A) experiment A, (B) experiment B, and (C) experiment C. Experiments A and B were performed using the same batch of cell extract, while experiment C was performed using a different batch of extract.

experiments suggests that the distribution of plasmids among wells is not the cause of the observed expression efficiency

dx.doi.org/10.1021/sb400028c | ACS Synth. Biol. 2013, 2, 497−505

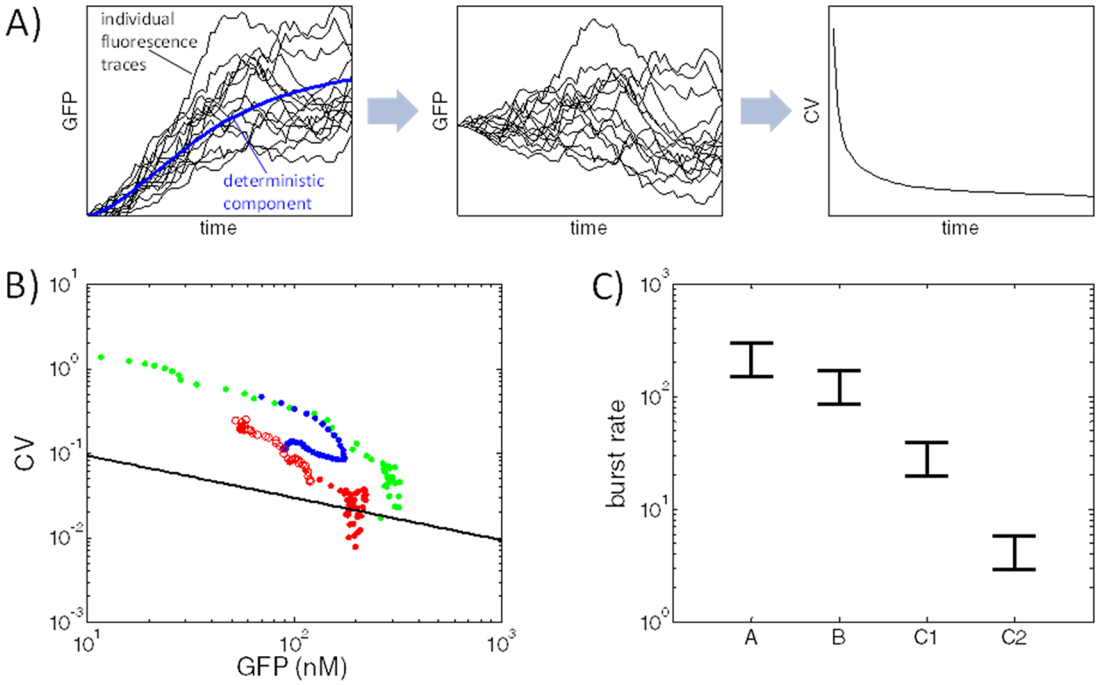

Figure 5. Noise calculations for expression experiments. (A) Starting with the fluorescence vs time traces from each microscopy experiment, we first calculate the deterministic component, which is based on the average of all expression trajectories. We then extract the noise and quantify how noise magnitude changes over time, which can be represented as the coefficient of variation (CV) vs time. (B) Average GFP vs time and CV vs time were calculated, and CV vs mean GFP was plotted for each time point for experiment A (green), experiment B (blue), experiment C, cluster 1 (red, open), and experiment C, cluster 2 (red, filled). The black line corresponds to a Poisson process for which the variance equals the mean. Each experiment initially exhibited significant deviation from a Poisson process, and the degree of deviation decreased over time. (C) On the basis of analysis of the noise data, we estimate burst factor ranges for each experiment.

variation. Interestingly, an unexpected non-Poissonian distribution of cell-free reagents has recently been observed in 100 nm scale vesicles[34] and in liposomes that are several μm in diameter.[33] This has been attributed to "spontaneous crowding" of expression machinery upon liposome formation, but the precise mechanism has yet to be elucidated.[41] Our observations in fabricated well arrays suggest that the phenomenon is not limited to liposomes and is rather a fundamental feature of protein expression components at the observed scale. Spontaneous crowding may also explain the qualitatively different behaviors observed among experiments A, B, and C, even when experiments are performed with the same cell extract batch and on the same day (experiments A and B). In particular, if this phenomenon occurs during the sealing of compartments, then the results would likely exhibit strong sensitivity to small variations in the setup process, such as the exact pressure used to seal the device.

Further investigation is required to identify which reaction components are distributed nonuniformly, and a possible approach would be to spike reactions with higher concentrations of different components. Ultimately, probing these biophysical phenomena of cell-free reactions at the micro scale will inform minimal cell and cell mimic efforts.[42−44] In addition, the question of whether such mixing or crowding effects occur in live cells has interesting implications in the partitioning of cell contents during division.[17,45,46]

Despite the different confined expression trends among the three experiments, several common observations are made. Within each experiment, expression efficiency varies significantly among the different wells. We rescaled the fluorescence vs time trajectories for each well and observed that the trajectories scale approximately multiplicatively with the ensemble average (Figure S2, SI). In other words, as shown in SI, the deterministic component of each of the M fluorescence trajectories $y_m(t)$ is well approximated by the average of all trajectories, $a(t)$, multiplied by a gain factor, G_m:

$$a(t) = \frac{1}{M}\sum_{m=0}^{M-1} y_m(t)$$

$$y_m(t) \approx G_m a(t)$$

In addition to the variation in expression efficiency among different wells, significant noise levels are observed within each well. To gain insight into the cell-free transcription and translation properties that give rise to the observed results, we extracted and analyzed gene expression noise for each experiment as depicted in Figure 5A. We first had to handle the fact that different wells have different expression efficiencies. On the basis of the multiplicative scaling of fluorescence vs time traces with the ensemble average (Figure S2, SI), we employed a rescaling technique[8] whereby noise for each well is determined by subtracting a scaled version of the ensemble average from the well's fluorescence vs time trace. In addition, since two distinct expression characteristics were observed in experiment C, fluorescence vs time characteristics were divided into two clusters using k-means clustering.[47] Cluster 1 (C1) corresponds to the trajectories in Figure 4C that exhibit strong initial expression, whereas cluster 2 (C2) corresponds to the trajectories that exhibit slow initial expression followed by an eventual increase.

Having extracted the noise, we then calculated noise magnitude. Noise magnitude can be represented as the

dx.doi.org/10.1021/sb400028c | ACS Synth. Biol. 2013, 2, 497−505

coefficient of variation (CV), which is defined as standard deviation of the noise divided by mean GFP (CV = σ/μ). Figure 5B shows the CV for each experiment, plotted at each time point as a function of the ensemble average GFP concentration at that time point. Figure 5B also shows the CV vs mean characteristic that would correspond to a Poisson distribution, for which the variance is equal to the mean ($\sigma^2 = \mu$). All experiments were observed to exhibit noise magnitudes greater than what would correspond to a Poisson distribution. Note that the CV vs GFP trend for Experiment B turns back on itself simply due to the eventual decrease observed in GFP expression. For all experiments, as shown in Figure S5, SI, the deviation from a Poisson process was observed to decrease over time as the expression rate presumably slowed down.

Another means of representing noise magnitude is the Fano factor η, which is defined as variance of the noise divided by mean GFP. Figure S5 in SI shows the Fano factor as a function of time for the same experiments. Fano factors greater than 1 were observed for all data sets, which further supports that each expression reaction deviates from a Poisson process. Data sets corresponding to higher expression levels were also observed to have higher peak Fano factors.

The noise calculations in Figure 5 provide insights into the properties of cell-free protein expression at the femtoliter scale. Cell-free expression kinetics often differ from in vivo expression kinetics,[48] and one interesting question is the extent to which cell-free expression reactions exhibit bursting. Both transcription and translation can potentially contribute to bursting. Transcriptional bursting arises from promoter transitions between active and inactive states, whereby bursts of mRNA are produced during active states.[19,49−51] While transcriptional bursting is observed for some *E. coli* promoters, it is far less pronounced than in eukaryotic systems.[52,53] Therefore, our analysis assumes that the deviations from Poisson distributions observed in Figure 5B are primarily attributed to translational bursting whereby several proteins are produced from each mRNA transcript. To further explain this, we consider the simple expression model in Table S1 in SI.

For translational bursting, the burst rate b is defined as the translation rate k_2 divided by the mRNA lifetime g_m, i.e. $b = k_2/g_m$. To estimate the burst rate values for the experimental data, we examine the continuous production model in Table S1, SI, which provides a reasonable approximation of the early measurements prior to the eventual decrease in expression rate. When the protein decay rate g_p is considerably slower than the mRNA decay rate g_m, such that g_p/g_m is negligible, the Fano factor dynamics are described as follows:[54]

$$\eta(t) = \left(\frac{1 - e^{-2g_p t}}{1 - e^{-g_p t}}\right) b + 1$$

Thus, the Fano factor settles from approximately $(2b+1)$ to a steady state value of approximately $(b + 1)$. When g_p/g_m cannot be neglected, the Fano factor typically peaks below $(2b + 1)$ and above the exact steady state given below:

$$\eta = 1 + \frac{k_2}{g_m + g_p}$$

Accordingly, to estimate the range of burst factors for each experiment on the basis of the peak Fano factors (η_p) observed in Figure S5, SI, we assume that b falls between $(\eta_p - 1)/2$ and $(\eta_p - 1)$. The apparent burst rates of the cell-free reactions (Figure 5C) are on the order of 10−100. This provides further support for our assumption that translation rather than transcription dominates the overall bursting behavior observed in our system. In particular, Taniguchi et al quantified Fano factors at the transcriptional level for 137 genes in *E. coli*, and the median Fano factor was 1.6.[53] Therefore, transcriptional bursting likely constitutes a minor contribution, if any, to the large burst rates that we find at the protein level. Interestingly, the burst rates that we observe in our cell-free system are on par with observed burst rates in *E. coli*.[53] However, it must be considered that mRNA half-life in the cell-free system that we used is 30−40 min,[55] which is roughly an order of magnitude greater than typical mRNA half-lives in live *E. coli*.[56] This suggests that translation rates are roughly an order of magnitude weaker in our cell-free reactions than in *E. coli*, which agrees with previous quantification of cell-free translation kinetics in bulk.[48,57]

We also note in Figure 5B that the deviations from Poisson behavior tend to diminish as the reactions proceed. This would suggest that the expression reactions slow down and eventually die out as a result of a decrease in the translation rate. As illustrated by the example model scenarios in Figure S4, SI, decreasing the transcription rate does not result in a decrease in the Fano factor, whereas decreasing the translation rate does cause a decrease in the Fano factor. The weaker translation rates that we observed in cell-free systems as compared to those in live cells, along with our finding that declining translation rates ultimately shorten cell-free expression lifetimes, hint at possible targets for improving cell-free reaction platforms. Of particular interest would be determining why translation rates are generally weaker in cell-free systems as well as developing methods for sustaining translation rates, for example through supplementation of specific cell-free components.

In this study, we showed that cell-free gene expression reactions can be compartmentalized in cell-scale volumes for the purpose of studying gene expression noise. The resulting noise analysis highlighted intrinsic characteristics of constitutive gene expression, including natural variation in expression intensity, as well as differences in gene expression kinetics between live cells and cell-free systems. Using our approach, gene expression noise can be studied in the absence of complicating factors associated with living cells, such as growth, division, mutation, and microenvironment variation. This, in turn, facilitates the separation of intrinsic and extrinsic noise. Likewise, in contrast to both living cells and vesicle confinement, our approach has a strictly defined reaction volume. This minimizes differences due to cell−cell or vesicle−vesicle variation, which could obscure noise results. In the future, this same approach could also allow us to explore the effects of cell size and shape on the function of different synthetic gene circuits.[55] Finally, unlike experiments with living cells, our experiments begin with a well-defined initial condition of zero mRNA and protein molecules produced from the expressed gene circuit. This can be of interest in the study of switching time distributions in bet-hedging and decision circuits.[8,58,59] In addition, if combined with actuatable membranes and microfluidic on-chip reagent mixing, well-defined initial conditions can facilitate quantification of early expression events.[39] Although we characterized expression in 20 fL containers, smaller volumes can be achieved with e-beam lithography and even with photolithography. Extending these efforts in confining cell-free gene circuit reactions not only offers a new platform for testing theoretical predictions on the role of

dx.doi.org/10.1021/sb400028c | *ACS Synth. Biol.* 2013, 2, 497−505

stochastic noise but also aids efforts to directly harness cell-free systems for various synthetic biology applications.[60]

MATERIALS AND METHODS

Device Fabrication. Standard 100 mm silicon wafers were used as masters for PDMS micromolding using conventional contact alignment optical lithography. MicroPrime MP-P20 (Shin-Etsu MicroSi, Inc., Phoenix, AZ) was spin-coated as an adhesion promoter prior to the photoresist coating. As an etch mask, we used a positive resist SPR-955-CM-0.7 photoresist (Microchem Corp., Newton, MA). Both the adhesion promoter and photoresist were spin-coated at 2000 rpm for 45 s. Wafers were baked on a hot plate at 90 °C for 90 s, exposed for 3.5 s, followed by a postexposure bake on a hot plate at 115 °C for 90 s. The development process was carried out in CD26 developer (5% tetramethylammonium hydroxide, MicroChem Corp., Newton, MA) for 1 min, rinsed with deionized water, and dried with nitrogen. A one-minute exposure to O_2−Ar plasma at 500 W (PVA Tepla Ion Wave 10) was conducted to remove any resist residue left on the exposed areas.

The patterned wafers were etched using a silicon waveguide etching process in an inductively coupled plasma ion etching system (Oxford Plasmalab 100). The process was carried out in a mixture of 60 sccm C4F8, 25 sccm SF6, and 2 sccm Ar gases at 20 °C, 15 mTorr and 30W RF. A 15-min etching time produced an etch depth of 2.8 μm, as measured by a Dektak profilometer. Removal of the photoresist was accomplished by soaking the substrate in *n*-methyl-pyrrolidinone (NMP 1165) (Microchem Corp., Newton, MA) at 70 °C, followed by exposure to 10 min oxygen plasma at 600 W.

PDMS devices were molded from the silicon masters. The silicon wafers were first silanized with trimethylchlorosilane vapor (Aldrich) for 1 h. The silanized wafer was then placed in an 11 cm diameter glass dish, and 55 g of degassed Sylgard 184 PDMS (Dow Corning) mixed according to manufacturer instructions was then poured over the wafer. After further degassing, the PDMS was set on a floating table at room temperature for overnight curing. Following room temperature curing, the device was cured for an additional hour at 70 °C.

Cell-Free Experiments. The Promega S30 T7 High-Yield Expression System was used for cell-free experiments. Cell-free reaction mixture was prepared by mixing S30 buffer with cell extract in a 10:9 ratio. This mixture was then added to Corning SpinX 0.22 μm spin columns and filtered by centrifugation for 1 min at 13200 rpm. The filtered mixture was first used for blocking to prevent adsorption of key reagents to the PDMS surface. A 5 μL aliquot was dispensed into a 35 mm Petri dish, and the device was placed onto the aliquot and allowed to sit for 15 min. Next, to prevent reactions from drying, the device was boiled for 30 min in Milli-Q purified water using a beaker cleaned with RNaseZap (Ambion). After cooling to room temperature, the surface of the device was dried using a tetrafluoroethane duster (Thorlabs). Then, 4 μL of filtered reaction mixture was mixed with 1 μL of 90 ng/μL pDEST17-EGFP DNA,[61] and 1 μL of this mixture was dispensed onto 22 mm × 22 mm No. 1 cover glass (Gold Seal). The device was then placed well-side down onto the mixture. Cellophane tape was placed on top of the device, and a 1.2 kg brass hex rod weight was also placed on top of the device for 10 min to aid sealing. The weight and tape were then removed, and a second piece of cover glass was placed on top of the PDMS to prevent drying. Imaging was then performed with the sample incubated at 30 °C.

Imaging. SEM images of the silicon masters and the PDMS replica shown in Figure 1 were carried out using the FEI Nova 600 scanning electron microscope. The PDMS device was coated with 50 nm of chromium prior to imaging to create a conductive path. For the cell-free experiments, fluorescent imaging was performed on a Zeiss LSM 700 confocal microscope with an incubation chamber set at 30 °C and a 63× oil objective. EGFP gain was set to 700, the maximum pinhole setting was used, zoom was set to 0.6, speed was set to 6, line averaging was set to 4, and laser power was set to 5%. Images (16 bit, 512 × 512 pixels) were captured every 5 min.

Image Processing. Images were processed in Image J[62] using the Time Series Analyzer plug-in. Fluorescence intensity values were converted to GFP concentrations on the basis of a calibration curve. This calibration curve was constructed by imaging the device loaded with different predefined concentrations of purified EGFP mixed with cell extract. Purified EGFP used in control experiments was prepared as previously described.[61]

Noise Analysis. We analyzed 144 fluorescence traces for Experiment A, 151 traces for Experiment B, and 223 traces for Experiment C. Experiment C traces were then divided into 177 traces for Cluster 1 and 46 traces for Cluster 2. Full details of the noise extraction and analysis are covered in the SI. Briefly, for noise extraction, we applied a previously developed method[8] to handle the fact that each trajectory corresponds to a different expression efficiency, which is captured through a gain term G_m as described above. To estimate noise magnitude, we developed an approach for filtering out white noise pollution due to autofocus error and measurement error on the microscope. As described in the SI, for each window, we approximated the noise variance $E[n(t)^2]$ as $E[n(t)n(t+1)]$. This is a reasonable approximation, since the sampling time is significantly lower than the half-lives of mRNA and GFP.[55] The approximation filters out the white component of the noise, since $E[n_{\text{white}}(t)n_{\text{white}}(t+1)] = 0$ by the definition of white noise.

ASSOCIATED CONTENT

Supporting Information

Details of cell-free expression measurement and noise analysis. This material is available free of charge via the Internet at http://pubs.acs.org.

AUTHOR INFORMATION

Corresponding Author

* Tel: (865)-574-8588 Fax: (865)-574-1753. E-mail: simpsonml1@ornl.gov.

Author Contributions

D.K.K. and S.Y.J. designed experiments. D.K.K. and S.Y.J. conducted experiments. B.S. and D.K.K. fabricated silicon masters. D.K.K. analyzed results. D.K.K., C.P.C., and M.L.S. interpreted results. All authors contributed to the manuscript preparation.

Notes

The authors declare no competing financial interest.

ACKNOWLEDGMENTS

We thank Dr. Roy Dar, Dr. Scott Retterer, Dr. Jennifer Morrell-Falvey, and Dr. Mitch Doktycz for helpful advice and conversations. We acknowledge support from the Center for Nanophase Materials Sciences that is sponsored by the

Scientific User Facilities Division, Office of Science, U.S. Department of Energy. This research was performed at Oak Ridge National Laboratory (ORNL). ORNL is managed by UT-Battelle, LLC, for the U.S. Department of Energy under contract DE-AC05-00OR22725.

REFERENCES

(1) Klammt, C., Löhr, F., Schäfer, B., Haase, W., Dötsch, V., Rüterjans, H., Glaubitz, C., and Bernhard, F. (2004) High level cell-free expression and specific labeling of integral membrane proteins. *Eur. J. Biochem. 271*, 568−580.

(2) Wong, R. W., and Blobel, G. (2008) Cohesin subunit SMC1 associates with mitotic microtubules at the spindle pole. *Proc. Natl. Acad. Sci. U.S.A. 105*, 15441−15445.

(3) Algire, M. A., Maag, D., Savio, P., Acker, M. G., Tarun, S. Z., Jr., Sachs, A. B., Asano, K., Nielsen, K. H., Olsen, D. S., Phan, L., Hinnebusch, A. G., and Lorsch, J. R. (2002) Development and characterization of a reconstituted yeast translation initiation system. *RNA 8*, 382−397.

(4) Iizuka, N., Najita, L., Franzusoff, A., and Sarnow, P. (1994) Cap-dependent and cap-independent translation by internal initiation of mRNAs in cell extracts prepared from Saccharomyces cerevisiae. *Mol. Cell. Biol. 14*, 7322−7330.

(5) Simpson, M. L., Cox, C. D., Allen, M. S., McCollum, J. M., Dar, R. D., Karig, D. K., and Cooke, J. F. (2009) Noise in biological circuits. *Wiley Interdiscip. Rev. Nanomed. Nanobiotechnol. 1*, 214−225.

(6) Fraser, D., and Kaern, M. (2009) A chance at survival: gene expression noise and phenotypic diversification strategies. *Mol. Microbiol. 71*, 1333−1340.

(7) Kittisopikul, M., and Suel, G. M. (2010) Biological role of noise encoded in a genetic network motif. *Proc. Natl. Acad. Sci. U.S.A. 107*, 13300−13305.

(8) Weinberger, L. S., Dar, R. D., and Simpson, M. L. (2008) Transient-mediated fate determination in a transcriptional circuit of HIV. *Nat. Genet. 40*, 466−470.

(9) Elowitz, M. B., Levine, A. J., Siggia, E. D., and Swain, P. S. (2002) Stochastic gene expression in a single cell. *Science 297*, 1183−1186.

(10) Balázsi, G., van Oudenaarden, A., and Collins, J. J. (2011) Cellular decision making and biological noise: From microbes to mammals. *Cell 144*, 910−925.

(11) Austin, D. W., Allen, M. S., McCollum, J. M., Dar, R. D., Wilgus, J. R., Sayler, G. S., Samatova, N. F., Cox, C. D., and Simpson, M. L. (2006) Gene network shaping of inherent noise spectra. *Nature 439*, 608−611.

(12) Simpson, M. L., Cox, C. D., and Sayler, G. S. (2003) Frequency domain analysis of noise in autoregulated gene circuits. *Proc. Natl. Acad. Sci. U.S.A. 100*, 4551−4556.

(13) Weinberger, L. S., Burnett, J. C., Toettcher, J. E., Arkin, A. P., and Schaffer, D. V. (2005) Stochastic gene expression in a lentiviral positive-feedback loop: HIV-1 Tat fluctuations drive phenotypic diversity. *Cell 122*, 169−182.

(14) Arkin, A., Ross, J., and McAdams, H. H. (1998) Stochastic kinetic analysis of developmental pathway bifurcation in phage λ-infected Escherichia coli cells. *Genetics 149*, 1633−1648.

(15) Süel, G. M., Kulkarni, R. P., Dworkin, J., Garcia-Ojalvo, J., and Elowitz, M. B. (2007) Tunability and noise dependence in differentiation dynamics. *Science 315*, 1716.

(16) Blake, W. J., Balázsi, G., Kohanski, M. A., Isaacs, F. J., Murphy, K. F., Kuang, Y., Cantor, C. R., Walt, D. R., and Collins, J. J. (2006) Phenotypic consequences of promoter-mediated transcriptional noise. *Mol. Cell 24*, 853−866.

(17) Rosenfeld, N., Young, J. W., Alon, U., Swain, P. S., and Elowitz, M. B. (2005) Gene regulation at the single-cell level. *Science 307*, 1962−1965.

(18) Cox, C. D., McCollum, J. M., Allen, M. S., Dar, R. D., and Simpson, M. L. (2008) Using noise to probe and characterize gene circuits. *Proc. Natl. Acad. Sci. U.S.A. 105*, 10809−10814.

(19) Dar, R. D., Razooky, B. S., Singh, A., Trimeloni, T. V., McCollum, J. M., Cox, C. D., Simpson, M. L., and Weinberger, L. S. (2012) Transcriptional burst frequency and burst size are equally modulated across the human genome. *Proc. Natl. Acad. Sci. U.S.A. 109*, 17454−17459.

(20) Hasty, J., Pradines, J., Dolnik, M., and Collins, J. J. (2000) Noise-based switches and amplifiers for gene expression. *Proc. Natl. Acad. Sci. U.S.A. 97*, 2075−2080.

(21) Murphy, K. F., Adams, R. M., Wang, X., Balázsi, G., and Collins, J. J. (2010) Tuning and controlling gene expression noise in synthetic gene networks. *Nucleic Acids Res. 38*, 2712−2726.

(22) Cookson, N. A., Cookson, S. W., Tsimring, L. S., and Hasty, J. (2010) Cell cycle-dependent variations in protein concentration. *Nucleic Acids Res. 38*, 2676−2681.

(23) Rosenfeld, N., Young, J. W., Alon, U., Swain, P. S., and Elowitz, M. B. (2005) Gene regulation at the single-cell level. *Science 307*, 1962.

(24) Jelsbak, L., and Søgaard-Andersen, L. (1999) The cell surface-associated intercellular C-signal induces behavioral changes in individual Myxococcus xanthus cells during fruiting body morphogenesis. *Proc. Natl. Acad. Sci. U.S.A. 96*, 5031−5036.

(25) Davidson, C. J., and Surette, M. G. (2008) Individuality in bacteria. *Ann. Rev. Genet. 42*, 253−268.

(26) Stewart, E. J., Madden, R., Paul, G., and Taddei, F. (2005) Aging and death in an organism that reproduces by morphologically symmetric division. *PLoS Biol. 3*, e45.

(27) Hilfinger, A., and Paulsson, J. (2011) Separating intrinsic from extrinsic fluctuations in dynamic biological systems. *Proc. Natl. Acad. Sci. U.S.A. 108*, 12167−12172.

(28) Jewett, M. C., and Swartz, J. R. (2004) Substrate replenishment extends protein synthesis with an in vitro translation system designed to mimic the cytoplasm. *Biotechnol. Bioeng. 87*, 465−471.

(29) Fujiwara, K., and Shin-ichiro, M. N. (2013) Condensation of an additive-free cell extract to mimic the conditions of live cells. *PloS One 8*, e54155.

(30) Nevo-Dinur, K., Nussbaum-Shochat, A., Ben-Yehuda, S., and Amster-Choder, O. (2011) Translation-independent localization of mRNA in E. coli. *Science 331*, 1081−1084.

(31) Rudner, D. Z., and Losick, R. (2010) Protein subcellular localization in bacteria. *Cold Spring Harbor Perspect. Biol. 2*, No. a000307, DOI: 10.1101/cshperspect.a000307.

(32) Nomura, S. M., Tsumoto, K., Hamada, T., Akiyoshi, K., Nakatani, Y., and Yoshikawa, K. (2003) Gene expression within cell-sized lipid vesicles. *ChemBioChem 4*, 1172−1175.

(33) Nourian, Z., and Danelon, C. (2013) Linking genotype and phenotype in protein synthesizing liposomes with external supply of resources. *ACS Synth. Biol. 2*, 186−193.

(34) Pereira de Souza, T., Stano, P., and Luisi, P. L. (2009) The minimal size of liposome-based model cells brings about a remarkably enhanced entrapment and protein synthesis. *ChemBioChem 10*, 1056−1063.

(35) Okano, T., Matsuura, T., Kazuta, Y., Suzuki, H., and Yomo, T. (2012) Cell-free protein synthesis from a single copy of DNA in a glass microchamber. *Lab Chip 12*, 2704−2711.

(36) Raj, A., and van Oudenaarden, A. (2008) Nature, nurture, or chance: Stochastic gene expression and its consequences. *Cell 135*, 216−226.

(37) Kubitschek, H. E., and Friske, J. A. (1986) Determination of bacterial cell volume with the Coulter Counter. *J. Bacteriol. 168*, 1466−1467.

(38) Phillips, R. B., Kondev, J., Theriot, J., Orme, N., and Garcia, H. (2009) *Physical Biology of the Cell*, Garland Science: New York.

(39) Jung, S.-Y., Liu, Y., and Collier, C. P. (2008) Fast mixing and reaction initiation control of single-enzyme kinetics in confined volumes. *Langmuir 24*, 4439−4442.

(40) Rondelez, Y., Tresset, G., Tabata, K. V., Arata, H., Fujita, H., Takeuchi, S., and Noji, H. (2005) Microfabricated arrays of femtoliter chambers allow single molecule enzymology. *Nat. Biotechnol. 23*, 361−365.

(41) Luisi, P. L., Allegretti, M., Pereira de Souza, T., Steiniger, F., Fahr, A., and Stano, P. (2010) Spontaneous protein crowding in liposomes: A new vista for the origin of cellular metabolism. *ChemBioChem 11*, 1989−1992.
(42) Fletcher, B. L., Hullander, E. D., Melechko, A. V., McKnight, T. E., Klein, K. L., Hensley, D. K., Morrell, J. L., Simpson, M. L., and Doktycz, M. J. (2004) Microarrays of biomimetic cells formed by the controlled synthesis of carbon nanofiber membranes. *Nano Lett. 4*, 1809−1814.
(43) Noireaux, V., and Libchaber, A. (2004) A vesicle bioreactor as a step toward an artificial cell assembly. *Proc. Natl. Acad. Sci. U.S.A. 101*, 17669−17674.
(44) Siuti, P., Retterer, S. T., and Doktycz, M. J. (2011) Continuous protein production in nanoporous, picolitre volume containers. *Lab Chip 11*, 3523−3529.
(45) Huh, D., and Paulsson, J. (2010) Non-genetic heterogeneity from stochastic partitioning at cell division. *Nat. Genet. 43*, 95−100.
(46) Huh, D., and Paulsson, J. (2011) Random partitioning of molecules at cell division. *Proc. Natl. Acad. Sci. U.S.A. 108*, 15004−15009.
(47) Seber, G. A. F. (1984) *Multivariate Observations*, Vol. *41*, Wiley: New York.
(48) Karzbrun, E., Shin, J., Bar-Ziv, R. H., and Noireaux, V. (2011) Coarse-grained dynamics of protein synthesis in a cell-free system. *Phys. Rev. Lett. 106*, 048104.
(49) Blake, W. J., Kærn, M., Cantor, C. R., and Collins, J. J. (2003) Noise in eukaryotic gene expression. *Nature 422*, 633−637.
(50) Dar, R. D., Karig, D. K., Cooke, J. F., Cox, C. D., and Simpson, M. L. (2010) Distribution and regulation of stochasticity and plasticity in Saccharomyces cerevisae. *Chaos 20*, No. 037106, DOI: 10.1063/1.3486800.
(51) Simpson, M. L., Cox, C. D., and Sayler, G. S. (2004) Frequency domain chemical Langevin analysis of stochasticity in gene transcriptional regulation. *J. Theor. Biol. 229*, 383−394.
(52) So, L.-h., Ghosh, A., Zong, C., Sepulveda, L. A., Segev, R., and Golding, I. (2011) General properties of transcriptional time series in Escherichia coli. *Nat. Genet. 43*, 554−560.
(53) Taniguchi, Y., Choi, P. J., Li, G.-W., Chen, H., Babu, M., Hearn, J., Emili, A., and Xie, X. S. (2010) Quantifying E. coli proteome and transcriptome with single-molecule sensitivity in single cells. *Science 329*, 533−538.
(54) Thattai, M., and van Oudenaarden, A. (2001) Intrinsic noise in gene regulatory networks. *Proc. Natl. Acad. Sci. U.S.A. 98*, 8614−8619.
(55) Karig, D. K., Iyer, S., Simpson, M. L., and Doktycz, M. J. (2012) Expression optimization and synthetic gene networks in cell-free systems. *Nucleic Acids Res. 40*, 3763−3774.
(56) Bernstein, J. A., Khodursky, A. B., Lin, P. H., Lin-Chao, S., and Cohen, S. N. (2002) Global analysis of mRNA decay and abundance in Escherichia coli at single-gene resolution using two-color fluorescent DNA microarrays. *Proc. Natl. Acad. Sci. U.S.A. 99*, 9697−9702.
(57) Underwood, K. A., Swartz, J. R., and Puglisi, J. D. (2005) Quantitative polysome analysis identifies limitations in bacterial cell-free protein synthesis. *Biotechnol. Bioeng. 91*, 425−435.
(58) Acar, M., Mettetal, J. T., and van Oudenaarden, A. (2008) Stochastic switching as a survival strategy in fluctuating environments. *Nat. Genet. 40*, 471−475.
(59) Çağatay, T., Turcotte, M., Elowitz, M. B., Garcia-Ojalvo, J., and Süel, G. M. (2009) Architecture-dependent noise discriminates functionally analogous differentiation circuits. *Cell 139*, 512−522.
(60) Hockenberry, A. J., and Jewett, M. C. (2012) Synthetic in vitro circuits. *Curr. Opin. Chem. Biol. 16*, 253−259.
(61) Retterer, S. T., Siuti, P., Choi, C.-K., Thomas, D. K., and Doktycz, M. J. (2010) Development and fabrication of nanoporous silicon-based bioreactors within a microfluidic chip. *Lab Chip 10*, 1174−1181.
(62) Schneider, C. A., Rasband, W. S., and Eliceiri, K. W. (2012) NIH Image to ImageJ: 25 years of image analysis. *Nat. Methods 9*, 671−675.